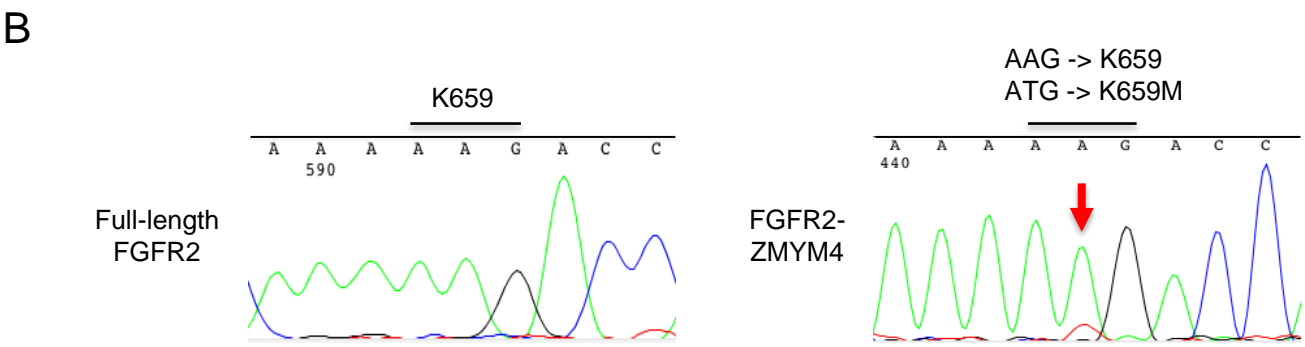
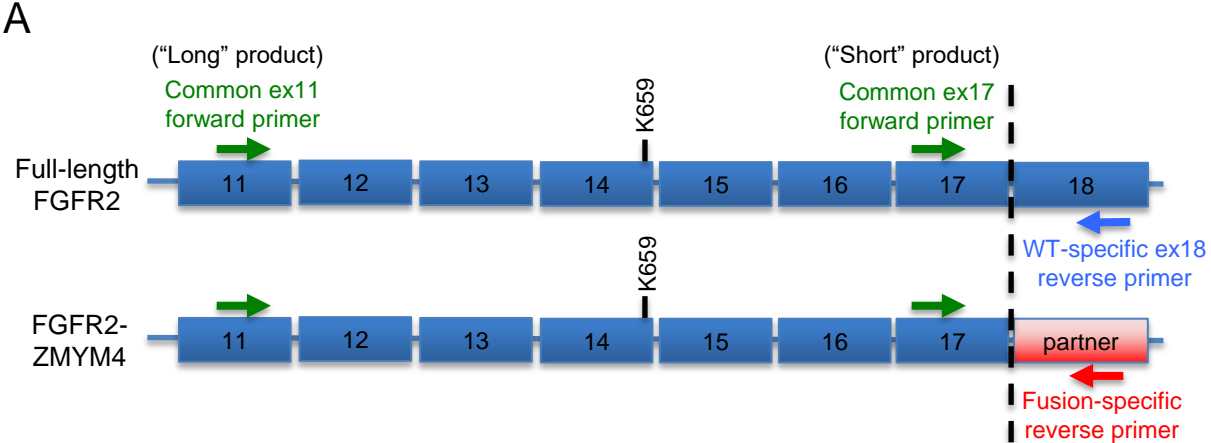


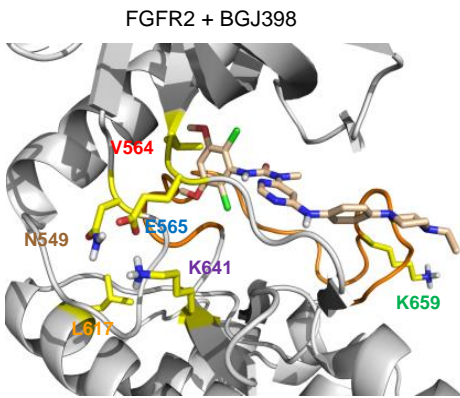
Supplementary Figure S1



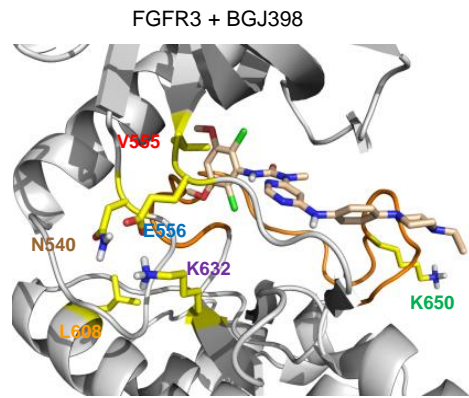
Supplementary Figure S1. Confirmation of secondary point mutation in FGFR2-ZMYM4 allele. A. Primers were designed to specifically amplify either full-length FGFR2 or FGFR2-ZMYM4 mRNA from post-progression biopsy tissue of Patient #1. **B.** Sequencing traces from Sanger sequencing demonstrates a K659M mutation in the FGFR2-ZMYM4 allele and not the full-length FGFR2 allele.

Supplementary Figure S2

A



B



C

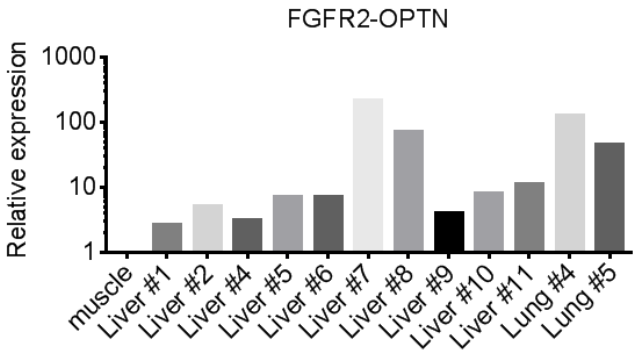
FGFR2	DKLTLGKPLGEGCFGQVVM AEAVGIDKDKPKEAVTVAVKMLKDDATEKDL
	.: : : : : : : : : :
FGFR3	ARLTLGKPLGEGCFGQVVM AEAI GIDKDRAAKPVTVAVKMLKDDATDKDL
FGFR2	SDLVSEMEMMKMIGKHKNI I ⁵⁴⁹ NLLGACTQDGPLYVIVE ^{564 565} YASKGNLREYLRA
	: : : : : : : : :
FGFR3	SDLVSEMEMMKMIGKHKNI I NLLGACTQGGPLYVLVEYAAKGNLREFLRA
FGFR2	RRPPGMEYSYDINRVPEEQMTFKDLVSC ⁶¹⁷ TYQLARGMEYLASQKCIHRDLA
	: : : : : : : : :
FGFR3	RRPPGLDYSFDTCKPPEEQMTFKDLVSCAYQVARGMEYLASQKCIHRDLA
FGFR2	ARNVLVTENNVM ⁶⁴¹ KIADFG ⁶⁵⁹ LARDINNIDYYKKT ⁶⁵⁹ TNGRLPVKWM APEALFDR
	: : : : : : : : :
FGFR3	ARNVLVTEDNVMKIADFG LARDVHNLDYYKKT TNGRLPVKWM APEALFDR
FGFR2	VYTHQSDVWSFGVLMWEI FTLGGSPYPGIPVEELFKLLKEGHRMDKPANC
	: : : : : : : : :
FGFR3	VYTHQSDVWSFGVLLWEI FTLGGSPYPGIPVEELFKLLKEGHRMDKPANC
FGFR2	TNELYMMRDCWHAVPSQRPTFKQLVEDLDRILTLTNEE
	: : : : : : : : : : :
FGFR3	THDLYMIMRECWHAAAPSQRPTFKQLVEDLDRVLTVTSTDE

Supplemental Figure S2: Homology between FGFR2 and FGFR3 proteins

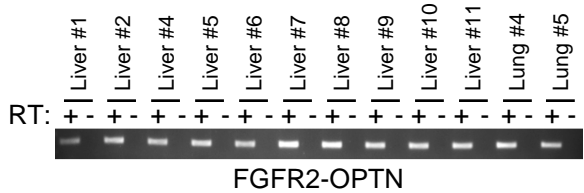
A and B. *In silico* model of wild-type FGFR2 (**A**) and FGFR3 (**B**) bound to BGJ398 with relevant amino acids highlighted and color-coded. **C.** Sequence alignment of FGFR2 and FGFR3 indicating sites of specific changes in amino acids due to FGFR kinase mutations.

Supplementary Figure S3

A



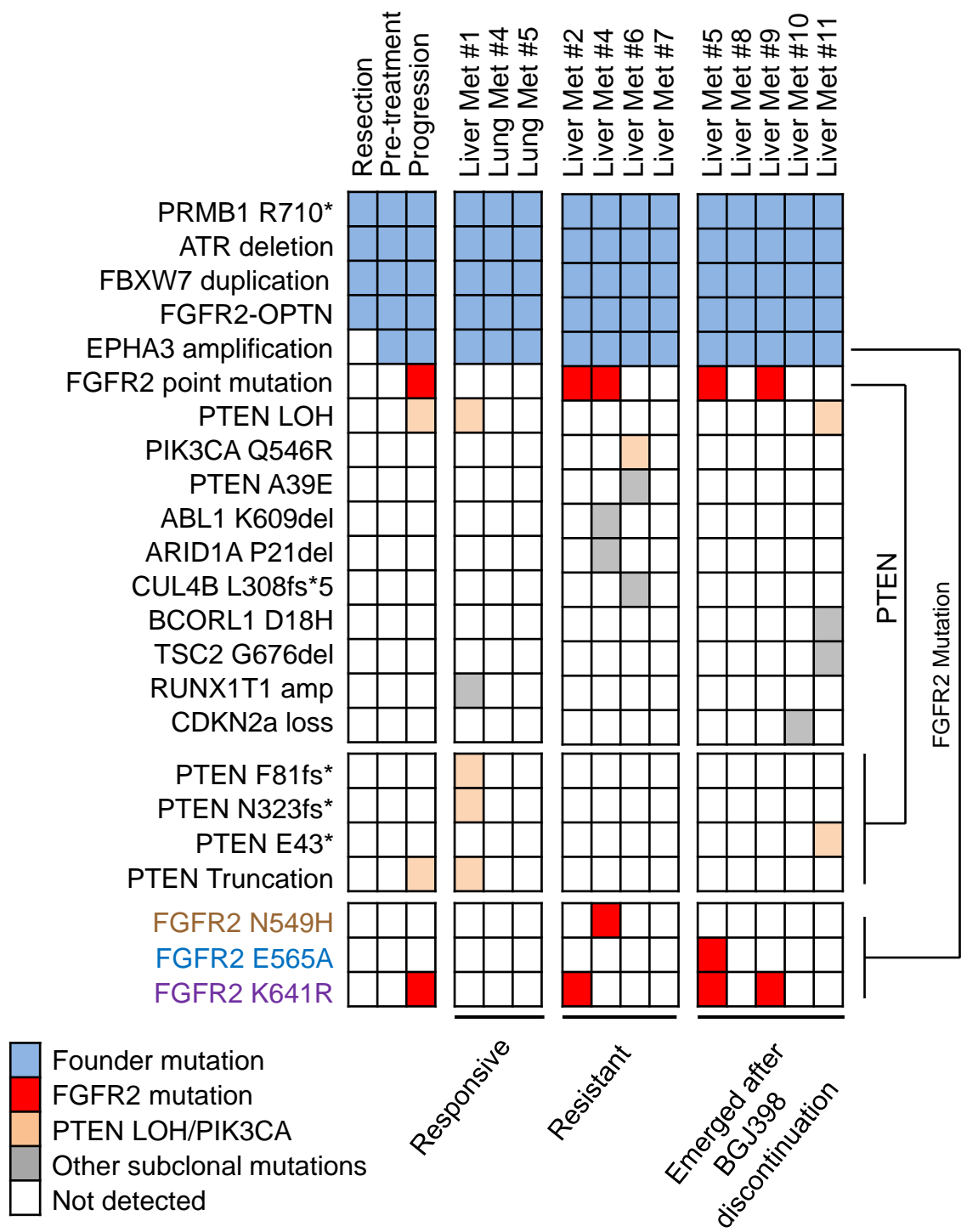
B



Supplementary Figure S3. FGFR2-OPTN fusion detected in all autopsy lesions.

A. Relative expression of the *FGFR2-OPTN* fusion in the indicated autopsy lesions as measured by real-time quantitative PCR (RT-qPCR). **B.** PCR product isolated from **A**, in the presence or absence of reverse transcriptase (RT), was resolved on an agarose gel.

Supplementary Figure S4



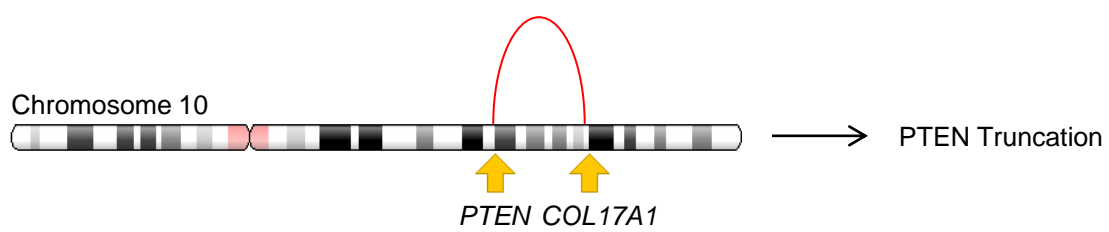
Supplementary Figure S4. FoundationOne analysis of autopsy lesions

Heatmap indicating all genetic events identified in the indicated Patient #2 lesions. Gray boxes indicate mutations of undetermined significance.

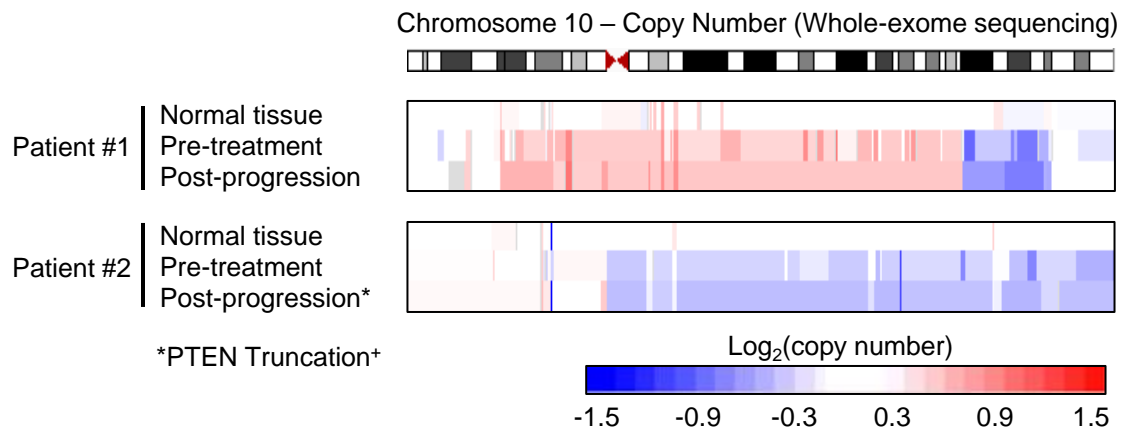
Supplementary Figure S5

A

Patient #2, Post-Progression Biopsy: FoundationOne analysis



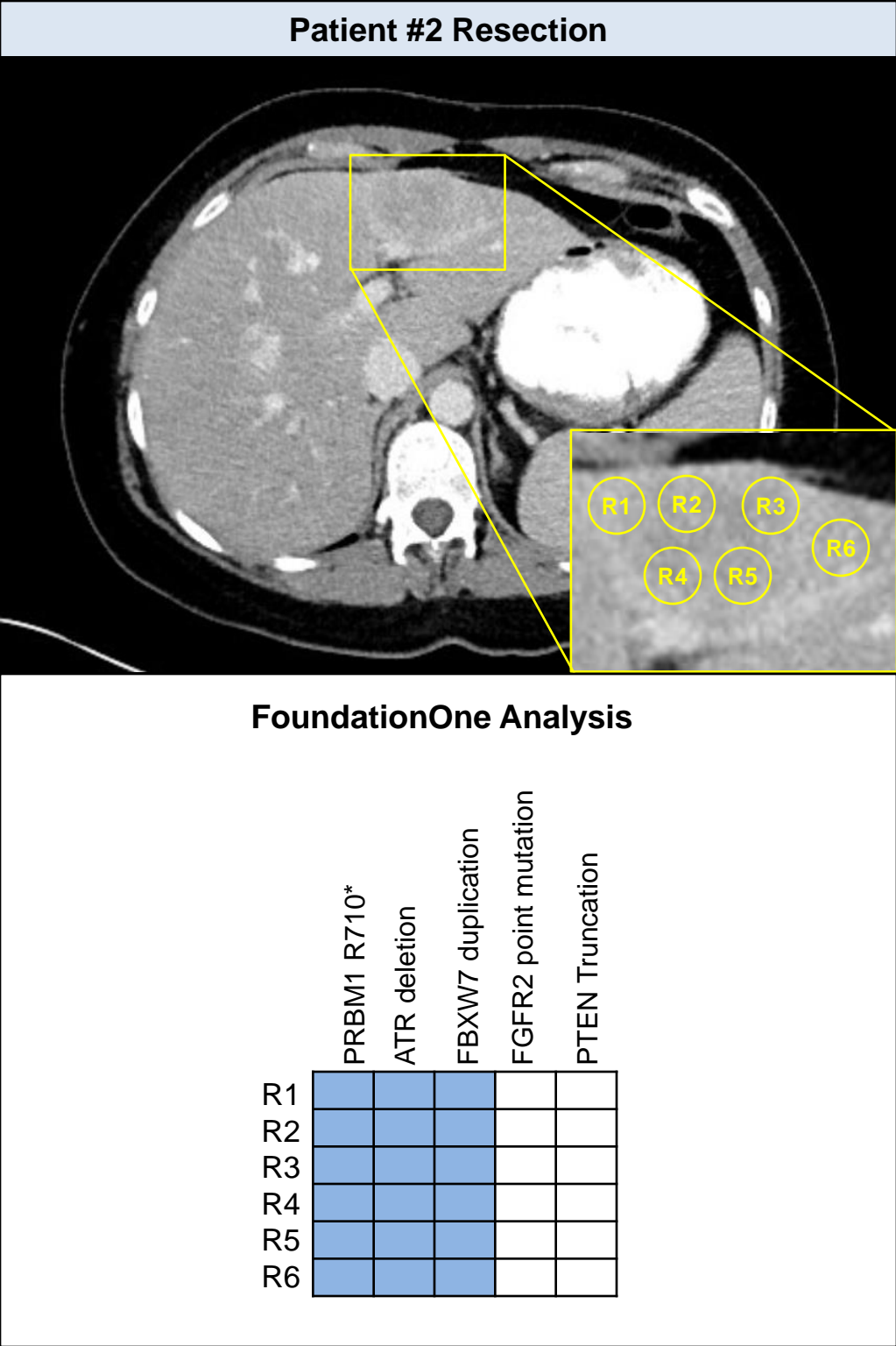
B



Supplementary Figure S5. *PTEN* loss of heterozygosity (LOH) identified in Patient #2.

A. Intrachromosomal fusion event detected by FoundationOne assay in the post-progression biopsy sample from patient #2 and leading to *PTEN* LOH. **B.** Heatmap illustrating the relative copy number along chromosome 10 in normal tissue, pre-treatment and post-progression biopsies from Patient #1 and Patient #2 as determined by WES. Note: Patient #2 demonstrates loss of the entire long arm of chromosome 10q as an early event (pre-treatment).

Supplementary Figure S6



Supplementary Figure S6. Mutational analysis of original resection specimen from Patient #2. *Top panel*, Axial contrast enhanced CT image of resected lesion from Patient #2. *Bottom panel*, Heatmap illustrating detected mutations in six spatially distinct pieces isolated from the resection specimen by FoundationOne assay.